LAWRENCE
LIVERMORE
NATIONAL
LABORATORY

LLNL-CONF-675135

Disposable Blast Shields For Use On NIF Imaging Diagnostics

C. A. Smith, K. M. Wang, N. Masters

July 23, 2015

SPIE Optics + Photonics 2015
San Diego, CA, United States
August 9, 2015 through August 13, 2015

Disclaimer

Disposable Blast Shields For Use On NIF Imaging Diagnostics

Cal A. Smith[a], Karen M. Wang[b], and Nathan Masters[a]

[a]Lawrence Livermore National Laboratory, 7000 East Avenue, Livermore, CA USA
[b]Stanford University, Building 500 Room 501T, Palo Alto, CA USA

ABSTRACT

The NIFs 192 lasers can deliver 2 MJ of energy to Target Chamber Center (TCC) to produce environments not available in any other experimental laboratory. The NIFs ability to deliver such intense energy to a small volume causes harsh consequences to experimental equipment and supporting diagnostics such as holhraums, support packages, target positioners, diagnostic equipment, and laser optics. Of these, the hohlraum and support packages are typically quickly vaporized and transformed into an expanding shell of high-hypersonic gases referred to as debris wind. During an experimental event such as fusion implosion, the target diagnostic components used to measure key observables in the experiment are subjected to extreme pressures and impact shocks due to incident debris wind loading. As diagnostics are positioned closer to TCC, the diagnostic pinhole stacks and other components along the diagnostic structure become more likely to be at or above the yield strength of the materials commonly used. In particular, the pinhole stack components and data recording instruments behind the pinholes are the most costly to replace. Thus, a conceptual configuration for a pinhole shield is proposed, analyzed, and tested with the intent of mitigating damage to the pinhole stack and imaging equipment and allowing immediate re-use of this diagnostic equipment. This pinhole shield would be a replaceable window that can be replaced quickly by inserting and removing it before and after each experimental laser shot, which will allow NIF to benefit from significant material and labor costs.

Keywords: NIF, disposable design, blast shield, pinhole protection

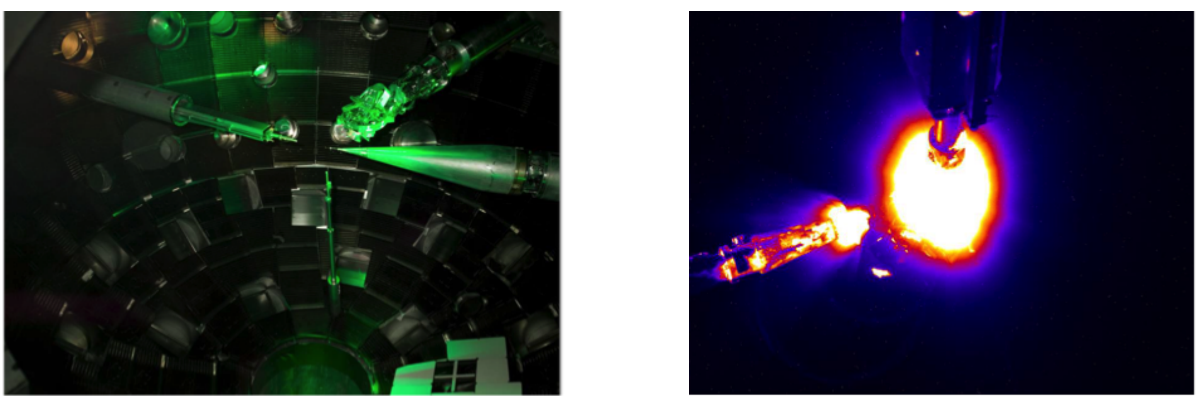

(a) View inside the NIF chamber. **(b)** Laser shot and resulting blast wave.

Figure 1: NIF chamber center with diagnositcs deployed.

Further author information:
E-mail: smith462@llnl.gov, Telephone: 925-423-4196
E-mail: kmwang14@stanford.edu, Telephone: 925-980-8649

This work was performed under the auspices of the U.S. Department of Energy by Lawrence Livermore National Laboratory under Contract DE-AC52-07NA27344.

1. INTRODUCTION

NIF diagnostics often use pinhole and collimator stacks at the front of the diagnostics to achieve increased sized images at the imaging plates of cameras. These pinhole and collimator plates are typically manufactured from tantalum or other X-ray blocking material so that only the desired photons are allowed to reach the detectors. During an experimental event such as fusion implosion, these pinholes and collimators are directly loaded by highly energized vaporized material expanding from the target, referred to as debris wind. Tantalum and tantalum-10 wt.% tungsten are the preferred materials for the pinhole and collimators because of their good strength and high ductility. These pinhole stack plates are typically deposited with hohlraum debris such as gold, plastics, aluminum, and other materials, as well as subjected to permanent yield deformation, leaving them unusable for future shots (See Figure 3). The components have close tolerance and small features that can be costly, and as the NIF continues to perform hundreds of experiments per year, the total cost could easily exceed $300,000. Extreme pressure shocks that occur over a short amount of time can be clearly seen from Figure 2. This hazard can yield, fail, and block pinholes caused by the debris wind. All these effects render the pinhole stack unusable since it can no longer serve its purpose to block unwanted X-ray and other signals. Furthermore, it may block the desired X-ray signals needed for passage through the pinholes themselves. Protection from these events are unique design challenges that the proposed concept aims to address.

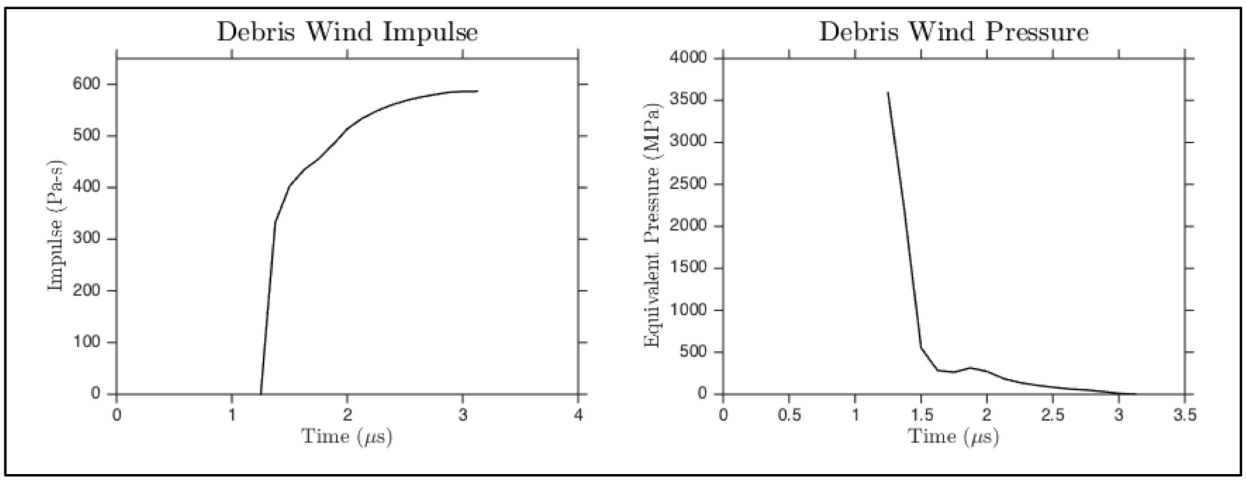

Figure 2: Typical Debris Wind profiles that occur during an experimental event.

Thus, it was proposed that an optically clear shield be placed in front of the pinhole stack to protect these expensive components from damage and allow their re-use. It was desirable to have them optically clear so that alignments could be made to the small holes in the plate. Furthermore, it was desired that the material not significantly block the photons of interest for the diagnostic.

2. MATERIAL SELECTION

Several materials such as beryllium, fused silica, and polycarbonate were considered in the design. Beryllium was considered since it has good strength and allowed much of the X-rays to pass through, but it was determined to be too brittle; surface damage would release small particularities of beryllium into the chamber, and this would be undesirable.[1] In addition, the material would not enable alignment of the pinholes directly, and a secondary alignment reference point would be needed. Fused silica was also considered since it would allow direct pinhole alignment,[2] but it was determined to be too brittle and its strength too low for its purpose.[3] Finally, polycarbonate was considered. Even though it would partially attenuate the photon signal, it would allow direct pinhole alignment. Furthermore, it has high ductility, which would enable it to be a very good energy absorber. Polycarbonate has been used in the NIF chamber for several purposes in the past and has shown to absorb debris wind loads through large plastic strain and displacements without failure. Since polycarbonate was determined to be a relatively inexpensive item, it could be designed to be a disposable item. The current diagnostics use layers of Kapton material as filters and debris protection, so it was postulated that if this Kapton were removed and replaced with the disposable polycarbonate debris window in the front, the overall effect on the diagnostic performance would not suffer greatly. Based on these reasons and experimental experience from the past, polycarbonate was chosen as the baseline material for the debris wind protective shield.

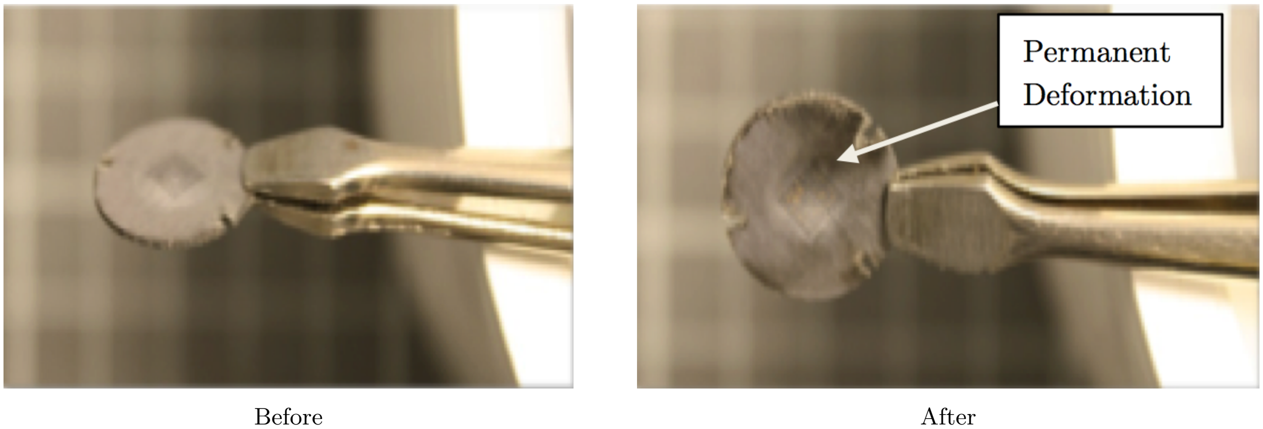

Figure 3: Damaged collimator component before and after an experimental event.

3. MODELING METHODOLOGY

Once the material was determined, several methods for positioning the polycarbonate in front of the pinhole stack were evaluated. Initially, different designs to support the polycarbonate window needed to be considered. In all concepts, a metallic nose cap was used to make the design as consistent with the operation and appearance of the current diagnostics. The nose cap was lengthened to allow the additional space required by the polycarbonate window.

In order to determine a suitable concept, the nose cap and polycarbonate piece were designed and analyzed using several different software packages. The nose cap and polycarbonate piece were meshed using a very fine, purely Lagrangian hexahedral mesh to capture the deformation and damage that was expected through the thickness due to the experimental event. Using both FEMAP and CUBIT, the nose cap and polycarbonate components where meshed with fine hexahedral solid elements (see Figure 4). The circular areas impacted by the debris wind were meshed using a butterfly meshing method with an even finer mesh at the center to better capture the effect of where the impact was expected to occur. The material models used were obtained from a database of verified models used by the lab. The main simulation software used to model the experimental event was LS-DYNA, an explicit dynamics finite-element software that specializes in simulating nonlinear dynamics,[4] impacts,[5] and blasts.[2] This software is used extensively in the automotive, aerospace, and military applications and has the capability to model events such as the high impact blast event seen in the NIF chamber. The results of the LS-DYNA simulations were verified using an in-house Arbitrary Lagrangian/Eularian solver developed at LLNL called ALE3D. The simulation produced results comparable to the LS-DYNA results to within several percent. Thus, the bulk of the simulations were done using LS-DYNA after confidence in the modeling methodology was established and cross-verified.

In order to model the experimental event, proper loading on the model needed to be applied. During an experimental event, the loading onto the polycarbonate window came primarily from target material that was vaporized and transformed into an expanding spherical shell of high-hypersonic gases referred to in the lab as debris wind. In addition to debris wind, the X-rays that are emitted from the experimental event ablate the polycarbonate material, resulting in an additional load. Although these events do not occur at the same time, both loads were conservatively added to the model over the debris wind time by applying a 1.1x multiplier to the debris wind load profile to account for the calculated force generated from ablation.[6]

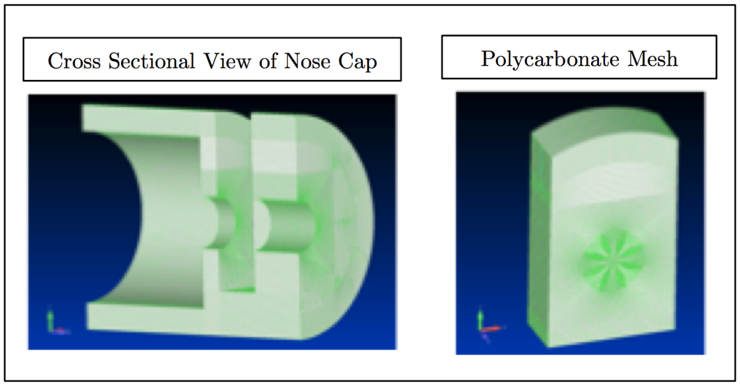

Figure 4: Meshed used in the polycarbonate debris window concept.

4. EARLY-STAGE DEVELOPMENT: SNAP RING CONCEPT

The initial concept used an internal snap ring to hold the polycarbonate window in place after it was inserted from the back of the nose cap (see Figure 5). The concept allowed for the nose cap tip to be screwed on so that the polycarbonate window assembly could be easily changed. Analysis showed that the snap ring would be required to be excessively thick in order to control its displacement and stress. All simulations showed the snap ring deforming substantially or rolling out of its retaining slot and local damage along the edge of the polycarbonate. The concept was determined to be too high of a risk since the behavior of the snap ring could not be adequately controlled under such dynamic environments. In addition, there was a possibility for thread damage on the front side of the cap, and this would create difficulty in removing the nose cap after an experimental shot. Another consideration was the implementation of the design; this concept would generate small and difficult to handle parts for the technicians. One critical lesson learned from this group of simulations was that providing a more compliant boundary for the polycarbonate window would reduce localized stresses around the perimeter of the window. This led to a larger polycarbonate component that extended well beyond the aperture of the diagnostic. Besides adding the needed compliance to the window support, a larger, easier to handle component that the technicians preferred was designed.

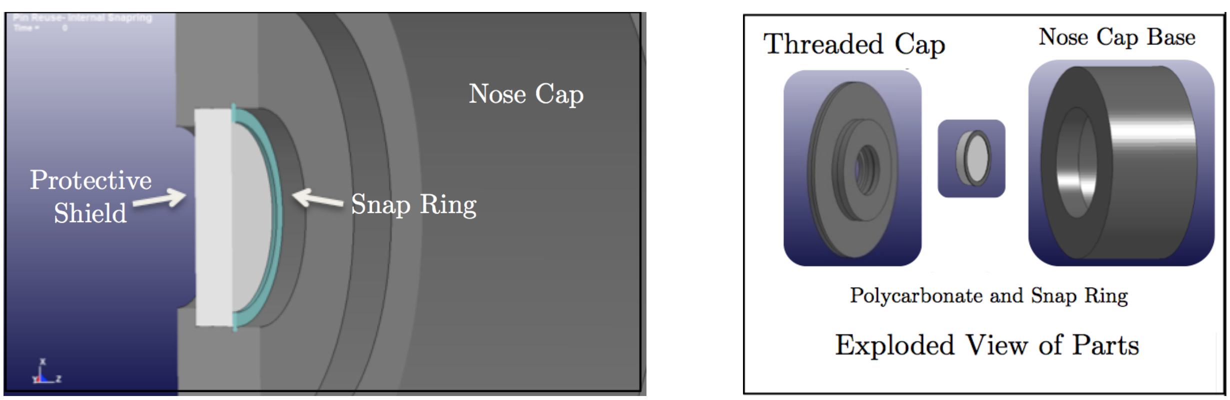

Figure 5: Snap ring support concept.

5. IMPROVED DESIGN DEVELOPMENT: SLOT CONCEPT

These ideas led to a nose cap which incorporated a large slot on the side to allow insertion of a single polycarbonate component. As a result, this required the nose cap to be manufactured from higher strength tantalum-10 wt.% tungsten (Ta10W) material to carry the localized bending and shear stresses generated by the debris wind impact on the assembly. This cap would have a side slot for insertion of a 4mm thick X 12mm X 20mm polycarbonate window component as is shown in Figure 6. In the simulations, the Ta10W for nose cap produced good strength results with low risk of yield and provided a stable slot for re-use of the nose cap for future shots. For the polycarbonate piece, a 4mm thickness was chosen to provide the ability to remove local material as needed for optimization of the aperture thickness, which is a function of the target mass and laser shot energy. To achieve the thickness optimization, the back surface of the polycarbonate was counter-bored to obtain the desired thickness in the aperture area needed for each shot. The resulting simulations showed high localized strains at the center of the polycarbonate window and along the edges of the counter-bore, especially along the edges where the nose cap aperture would be exposed to direct debris wind loading through the window. Some simulations showed complete plugging out of the center portion of the debris window with material traveling at speeds up to 350 m/s, while others showed material spallation off the back surface traveling at speeds of 50 m/s. Both of these failures were considered catastrophic since they would allow the pinhole stack to be loaded and possibly damaged. Based on these results, the windows were sized to produce a desired factor of safety of 2.0 to the apparent ultimate plastic strain of 70% to failure. This meant that up to 35% plastic strain was allowed in the open area of the window and overall physical deformation of the polycarbonate window. The counter-bore on the back side conveniently provided a space to allow this permanent deformation without causing interference with the nose cap slot during removal.

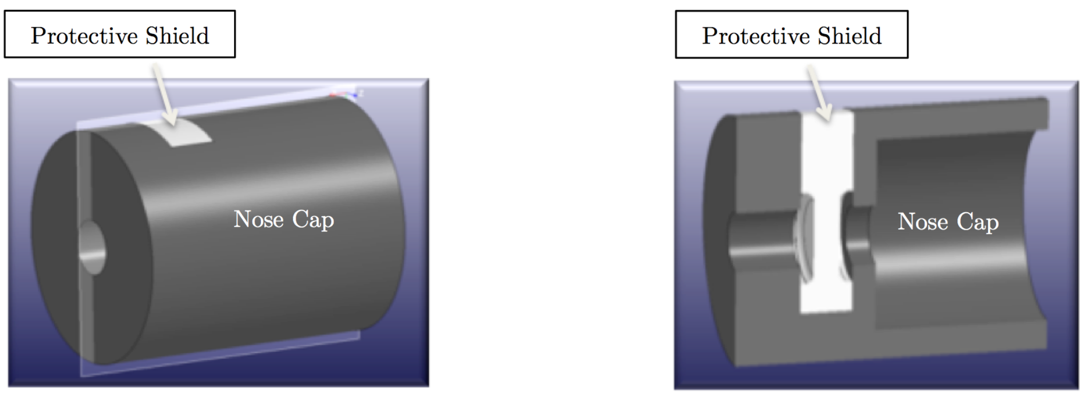

Slot Concept

Cross-Sectional VIew

Figure 6: Polycarbonate slot concept with nose cap.

Additionally, simulation results showed plastic strain as high as 55% localized around the edges of the polycarbonate aperture areas. This was determined to be caused by the sudden discontinuity between the thicknesses of the main window component and the counter-bored area. It was also noted that the stresses were higher near the sharp corners of the counter-bored region on the backside of the polycarbonate piece. Thus, an internal radius in the counter-bore was recommended in order to mitigate the stress concentration issues at the edges of the counter-bore. This also led to the recommendation that the counter-bore diameter be at least 1 mm larger than the nose cap aperture size and have a minimum internal radius on the counter-bore corner of 0.5 mm. The purpose of the internal radius was to resolve localized high strains by adding more compliance to the thinner section of the window and mitigate plugging out of the center area as seen in previous simulations. This larger diameter resulted in simulations that showed permanent deformation of the polycarbonate window of approximately 0.2-0.5 mm that were well within the depth of the back surface of the counter-bore. Futhermore, these changes allowed the polycarbonate to distribute the load over a broader area, causing damage to the piece to be less severe and more survivable, and as a result, the simulations showed less localized high strains along the perimeter of the piece.

There was additional concern of target material deposits building up on the front surface of the window and hindering the removal of the polycarbonate window from the nose cap slot. Thus, the addition of a counter-bore on the front surface at the center of the polycarbonate window with a diameter larger than the nose cap aperture was proposed to allow for the debris material deposition on the front side. The 4 mm total thickness of the window component allowed for both front and rear counter-bores to be used, and the purpose of these counter-bores were to provide both front surface material deposition growth and rear permanent deformation that was within both counter-bore volumes. Due to these constraints, the polycarbonate window was required to have at least a 0.5 mm counter bore on both the front surface and rear surface while allowing up to a 3 mm window section to remain in the aperture area for thickness optimization for each experimental laser shot. The new counter-bored window component design and its assembly to the nose cap can be seen in Figure 6 of the analysis model and Figure 7 of the initial prototype as a build component.

A series of analyses were performed to determine the range of window aperture thicknesses required to assure safe application with low risk of window catastrophic failure. This was an iterative approach to sizing the debris window for each instance, and the range of debris wind loading was based on non-ignition targets with 0.5 to 2.0 MJ of energy deposited on them at a distance of 10 cm from the target. These thicknesses are shown in Table 1. Although significant plastic strain was seen in simulations, a factor of 2.0 to ultimate plastic strain was maintained for all energies. During these simulations, it was observed that the window was vibrating out of its nose cap slot during the shot since it was unconstrained. In order to prevent this from happening, setscrews were added on the sides of the nose cap that mated with notches within the window. In addition, a push screw was added to the closed side of the slot for ease of removal out of the slot in case the polycarbonate piece became stuck in the nose cap due to deformation or debris deposits.

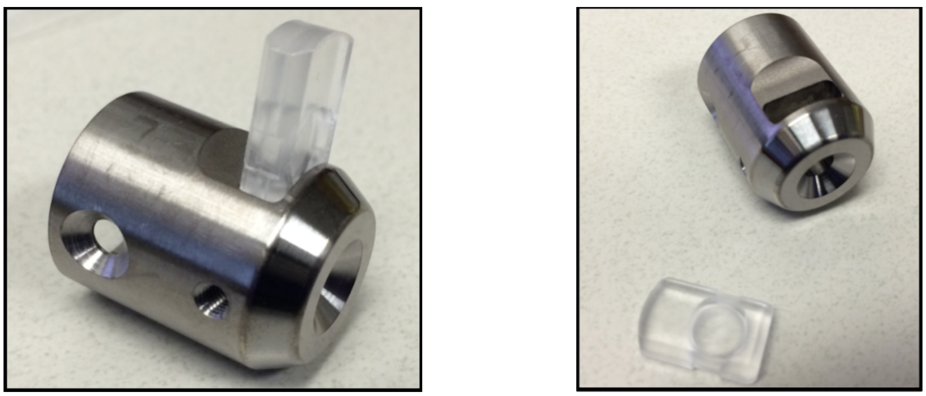

(a) Partially assembled to show the details of the parts. **(b)** Assembly is shown disassembled to show details of the parts.

Figure 7: First build of the debris window assembly. In the actual fielded part, the window would be fully inserted and locked in with side set screws. The optically clear polycarbonate piece and Ta10W silver nose cap pieces can be clearly seen in the pictures. Furthermore, holes for the set screw and push screw can be seen on the side of the nose cap.

Table 1: Optimized Polycarbonate window aperture thicknesses.

Expected Energy Range	Equatorial Diagnostic 90, 78 100 mm PH	Polar Diagnostic 0, 0 100 mm PH	
500 KJ - 1.0 MJ	1.0	1.5	
1.0 MJ - 1.25 MJ	1.25	1.9	Polycarbonate
1.25 MJ - 1.5 MJ	1.35	2.2	Thickness
1.5 MJ - 1.75 MJ	1.45	2.5	
1.75 MJ - 2.0 MJ	1.5	2.7	

Finally, the internal radius of the polycarbonate window was evaluated to see if other options would be possible and easier to manufacture. A chamfer concept versus a fillet concept was evaluated to determine whether a more gradual transition rather than a small local radius would be more effective. Simulation result showed that the chamfered concept tended to stiffen the window aperture, concentrating the loads and increasing the risk of higher plastic yielding. The chamfer was also found to have higher localized strains and material cracking on the edges compared to the fillet concept. Furthermore, the plastic strain seen on the front surface of the window was higher and penetrated deeper through the thickness of the window compared to the fillet concept. Thus, the fillet concept for the inner radius remained the recommended configuration. Figure 8 shows the final debris window configuration as manufactured and fielded for concept validation. It is important to note that although the components look large in the photo, they are still very small as can be evaluated by referencing the 4mm thickness of the window component. Both Figures 7 and 8 show the components partially installed to provided a clearer representation of the components in the assembly.

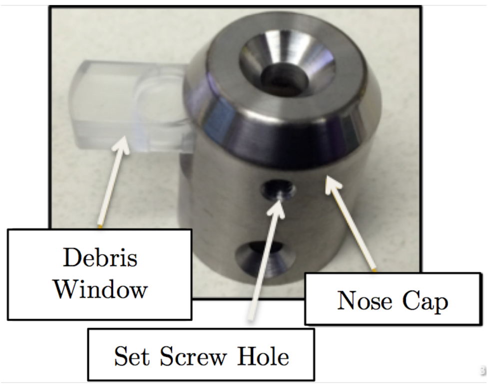

Figure 8: First build of the debris window assembly: polycarbonate slot concept with nose cap. The set screw hole shown will hold the debris window in place once it is fully installed.

In Figure 9, the expected results are observed. Although X-Ray ablation on the front surface with some material deposition and some deformation of the back surface can be seen, the validation shot was successful in showing no failures and fully protecting the pinhole stack.

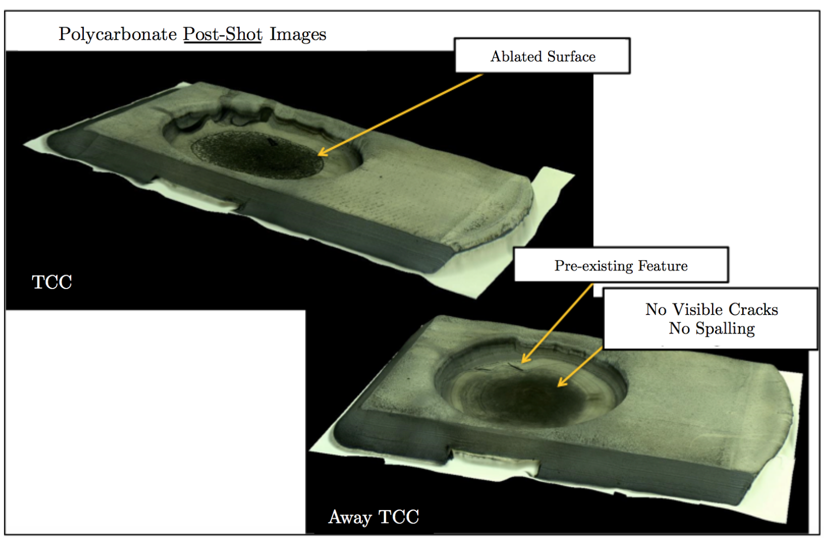

Figure 9: Post shot visual inspection.

Figure 10 shows a detailed deformation comparison between analysis and test, with excellent correlation. Based on this positive result, there is an effort to be more aggressive by thinning the window even more and accepting more risk. With increased confidence in the design, the debris window has been implemented on a large number of shots in NIF when allowed. Before reusing the pinhole, the entire area is carefully inspected in order to make sure there is no unexpected collateral damage. It is noted that there are conditions where the experimental requirements do not allow for the signal attenuation generated by the polycarbonate as discussed in Section 2, and in these cases, the pinhole stack continues to remain unprotected. Potential methods to address this issue include implementation of beryllium or polycarbonate encapsulated beryllium to see if lower attenuations of the X-Ray signal can be achieved.

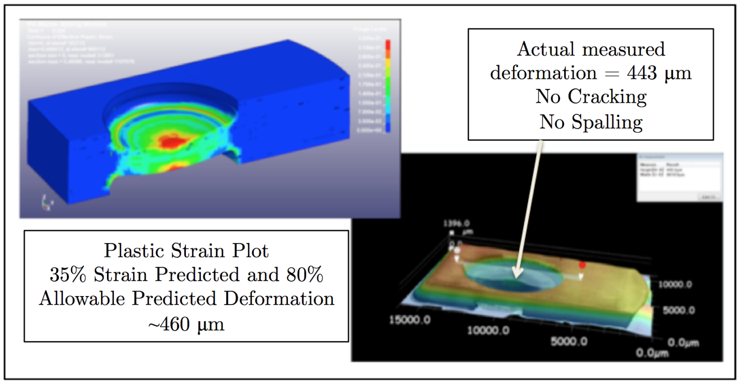

Figure 10: Post shot simulation validation.

6. CONCLUSION

Several concepts were considered in the design of the polycarbonate debris protective window, and a suitable design was found and tested. The final concept included a Ta10W nose cap with a side slot for insertion of a polycarbonate debris window. The design of the debris window included a front and rear oversized counter-bored aperture area with corner radii and set screws to hold it in place. It was observed that the Ta10W nose cap was not a design issue since it never showed any plastic strain even in the worst-case scenario. Although signs of carbon deposition on the pinhole stack has been observed due to ablation of the inner surface of the polycarbonate window, these carbon depositions have been minimal and are not a functional concern. A validation shot was performed, showing no failures and successfully protecting the pinhole stack. Confidence in the concept has led to increased use in the NIF chamber, and further improvements and riskier concepts are currently being developed.

ACKNOWLEDGMENTS

The authors would like to thank Jay Ayers, Robin Hibbard, and Kim Christensen, who helped in fielding the components for test and usage in scheduled experimental tests at NIF.

REFERENCES

[1] Wilson, D. C., Bradley, P. A., Hoffman, N. M., Swenson, F. J., Smitherman, D. P., Chrien, R. E., Margevicius, R. W., Thoma, D., Foreman, L. R., Hoffer, J. K., Goldman, S. R., Caldwell, S. E., Dittrich, T. R., Haan, S. W., Marinak, M. M., Pollaine, S. M., and Sanchez, J. J., “The development and advantages of beryllium capsules for the national ignition facility,” *Physics of Plasmas* **5** (1998).

[2] Zacharias, R., Beer, N., Bliss, E., Burkhart, S., Cohen, S., Sutton, S., Atta, R. V., Winters, S., Salmon, J., Stolz, C., Pigg, D., and Arnold, T., “National ignition facility alignment and wavefront control,” *Proceedings of SPIE* **5341** (2004).

[3] Milam, D., “Review and assessment of measured values of the nonlinear refractive-index coefficient of fused silica,” *Applied Optics* **37**(3) (1998).

[4] Livermore Software Technology Corporation, 2876 Waverley Way, Livermore, CA 94550, *LS-DYNA User’s Manual*, 950 ed. (May 1999).

[5] Borvik, T., Hopperstad, O., Berstad, T., and Langseth, M., "A computational model of viscoplasticity and ductile damage for impact and penetration," *European Journal of Mechanics and Solids* **20**, 285–712 (2001).

[6] Eder, D., Anderson, A., Braun, D., and Tobin, M., "Ablation of nif targets and diagnostic components by high power lasers and x rays from high temperature plasmas," *Proceedings of SPIE* **5341** (2004).